Supporting Information

Water quality–fisheries tradeoffs in a changing climate underscore the need for adaptive ecosystem–based management

Donald Scavia[a], , , Stuart A. Ludsin[b], Anna M. Michalak[c,d], Daniel R. Obenour[e], Mingyu Han[f], Laura T. Johnson[g,2], Yu-Chen Wang[h], Gang Zhao[i], and Yuntao Zhou[f]

[a] School for Environment and Sustainability, University of Michigan, Ann Arbor, MI 19350

[b] Aquatic Ecology Laboratory, Department of Evolution, Ecology, and Organismal Biology, The Ohio State University, Columbus, OH 43212

[c] Department of Global Ecology, Carnegie Institution for Science, Stanford, CA 94305

[d] Department of Earth System Science, Stanford University, Stanford, CA 94305

[e] Department of Civil, Construction & Environmental Engineering, NC State University, Raleigh, NC 27695

[f] School of Oceanography, Shanghai Jiao Tong University, Shanghai 200240, China

[g] National Center for Water Quality Research, Heidelberg University, Tiffin, OH 44883

[h] Hsinchu City 300, Taiwan

[I] Key Laboratory of Water Cycle and Related Land Surface Processes, Institute of Geographic Sciences and Natural Resources Research, Chinese Academy of Sciences, Beijing 100101, China

Contents Page

1. Overall modeling framework schematic

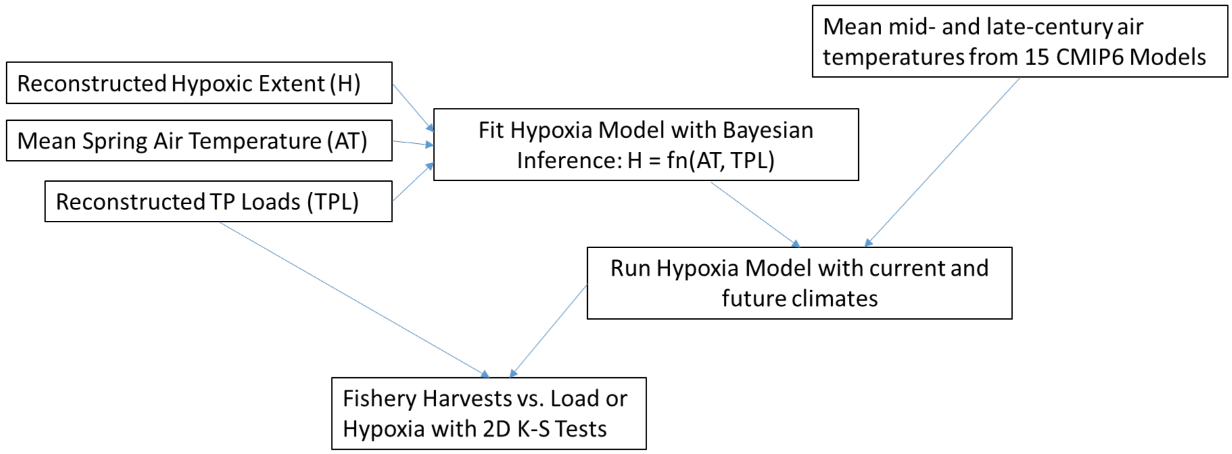

Figure S1. Conceptualization of the modeling framework used to reconstruct past bottom hypoxia extent, quantify threshold relationships between hypoxia and fisheries harvests, and project the anticipated effects of nutrient abatement and climate change on water quality and fishery yields in Lake Erie.

2. Hypoxia model development and supplemental hypoxia figures

Model testing - We tested the influence of several total phosphorus (TP) loading and air temperature intervals on bottom hypoxia. Del Giudice et al. (2018) reported a best fit using mean March-April air temperature and the cumulative tributary load from the previous 9 years. Using a similar model with our longer data record (that for the first time included the Detroit River), we also found that March-April mean air temperature and the cumulative TP load best predicted hypoxic extent. However, our model showed that loads from the previous 6 years plus October-May in the current year provided the best fit (Figure S2).

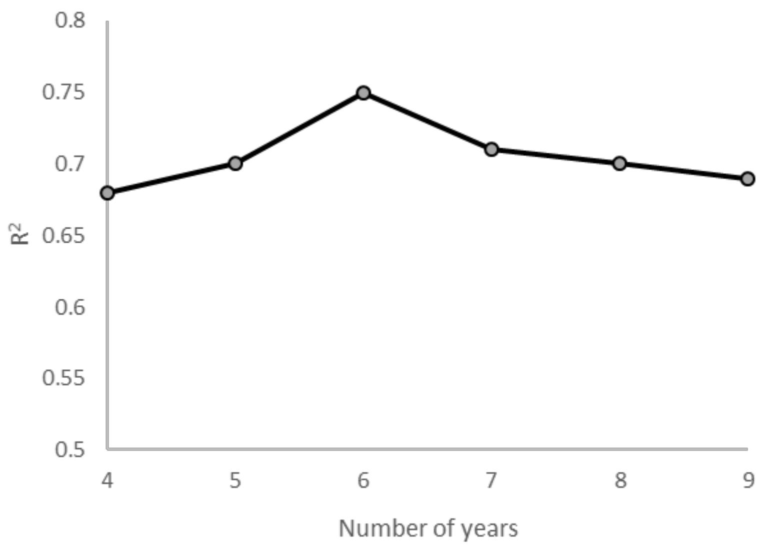

Figure S2. Comparison of R^2 values for the hypoxia model using different numbers of years in calculating the cumulative TP load to the central basin of Lake Erie.

We developed a Bayesian linear multiple regression model using the rstanarm package in R with Stan, as described in the main text. The model uses the previous years' cumulative TP load and the current year's March-April average temperature to predict the annual hypoxic area. Bayesian parameter estimation was conducted using four MCMC chains with 2,000 iterations, and the first 1,000 iterations being discarded as burn-in. All the model coefficients (parameters) reach convergence with an Rhat (potential scale reduction factor) smaller than 1.1. The tables below report the prior and posterior distributions for each coefficient.

Prior distributions for model coefficients

Coefficient	Distribution	Setting
Intercept	Normal	Location = 5.9, Scale = 3.3
March-April average temperature	Normal	Location = 0.7, Scale = 0.16
Cumulative TP load	Normal	Location = 0.0007, Scale = 0.00005
Sigma	Exponential	Rate = 0.3

Posterior distributions for model coefficients

Variable	Mean	Median	SD	5th Percentile	95th Percentile	Rhat
Intercept	-4.24	-4.26	0.63	-5.27	-3.18	1.00
March-April average temperature	0.71	0.71	0.11	0.52	0.89	1.00
Cumulative TP load	0.000698	0.000698	0.000037	0.000636	0.000757	1.00
Sigma	1.58	1.56	0.17	1.32	1.88	1.00

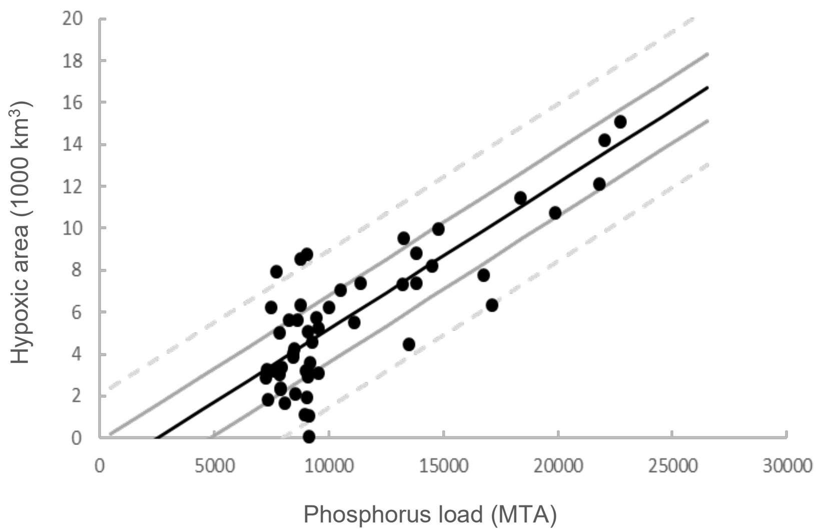

Figure S3. Bayesian hypoxia predictions versus phosphorus load in Lake Erie, 1959-2022. The 95% prediction intervals (gray dashed) and 60% prediction intervals (grey solid) are shown. Observed hypoxic areas are shown as black dots. Note that 1975, an outlier year (Figure 2) was removed from this model because the thermocline in 1975 was unusually shallow (DiToro et al, 1987; Rosa and Burns, 1987), which resulted in an exceptionally large hypolimnetic volume and dissolved oxygen mass. Instead of arbitrarily correcting for the larger volume to make the 1975 DO deletion rate consistent with other years, as in these other studies, removed the outlier.

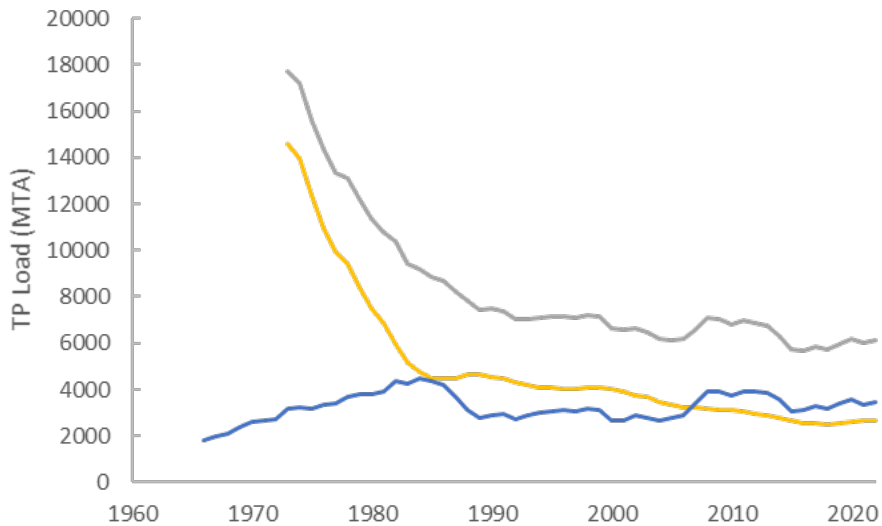

Figure S4. Total (grey), Detroit River (yellow), and tributary (blue) 6-year cumulative load, 1967-2020.

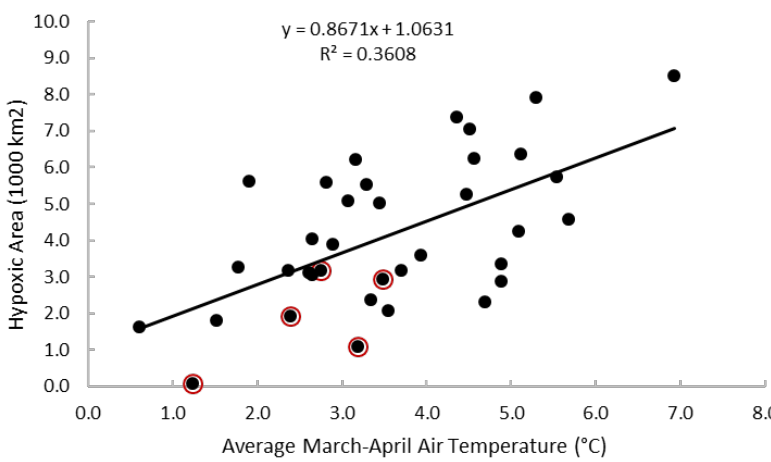

Figure S5. Relationship between 1985-2022 hypoxic area and average March-April air temperature. The 1993-1997 data points are circled to identify a period of very low air temperature.

3. Fisheries threshold determination

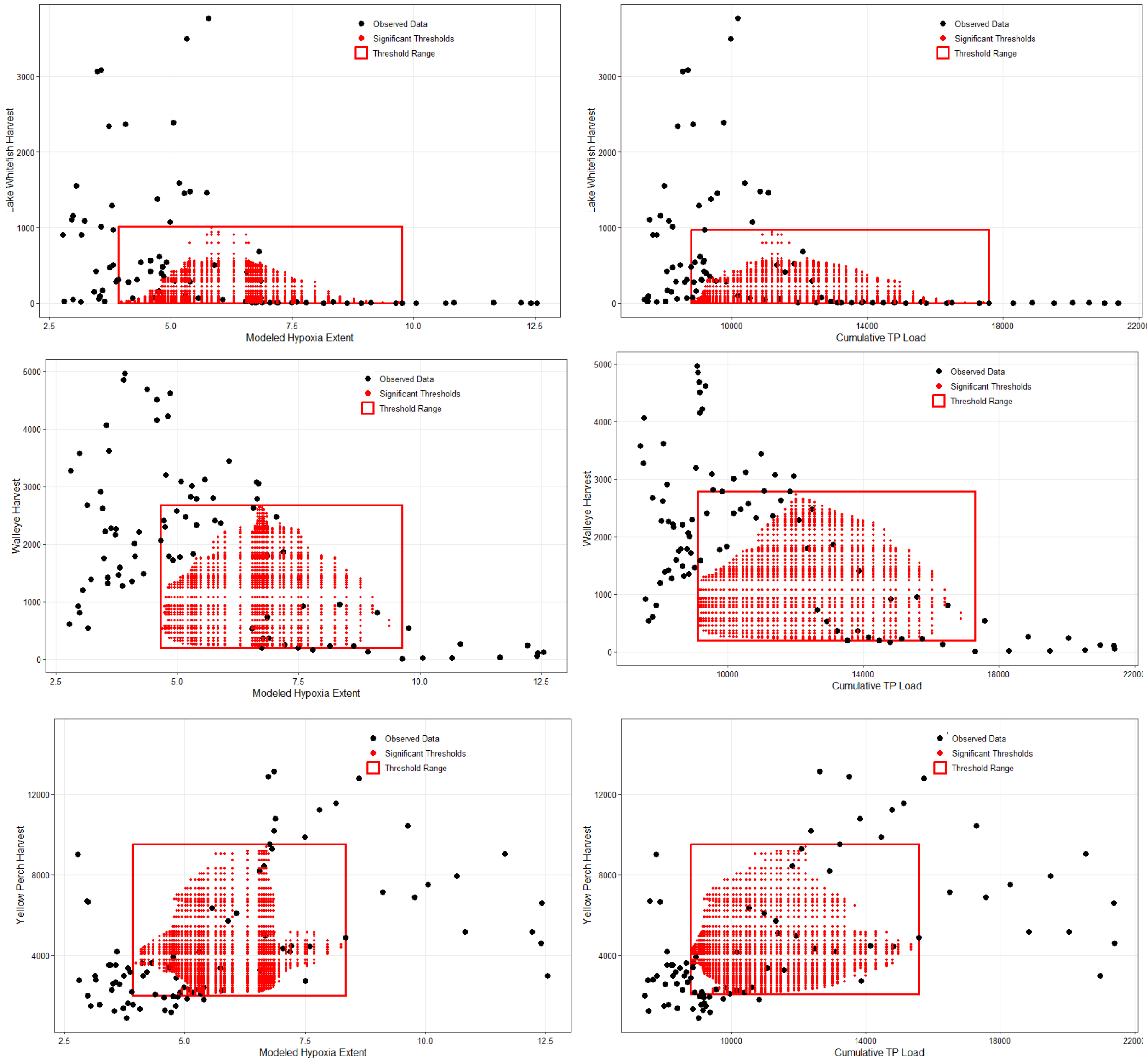

Figure S6. Results from two-dimensional Kolmogorov-Smirnov tests (Garvey et al., 1998) used to identify threshold relationships between Lake Whitefish (top panels), Walleye (middle panels), and Yellow Perch (bottom panels) commercial harvests and either hypoxia extent (5-year running means; left panels) or cumulative (6-year) total phosphorus loads (5-year-running means; right panels) during 1932-2020. Portrayed in each panel are observed data, all significant thresholds ($p < 0.05$) identified for every possible combination of the randomized data, and the range of the significant thresholds identified across all runs. Significance of each threshold identified in each randomization was determined by comparing the D value for that randomization against a null distribution of D values determined from 5,000 rerandomizations of the data. Randomizations were used to also determine 95% confidence intervals reported in the main text. Note: Fisheries harvest data are from the Great Lakes Fisheries Commission (http://www.glfc.org)

4. Temperature anomalies and variation in hypoxic thickness, extent, and duration

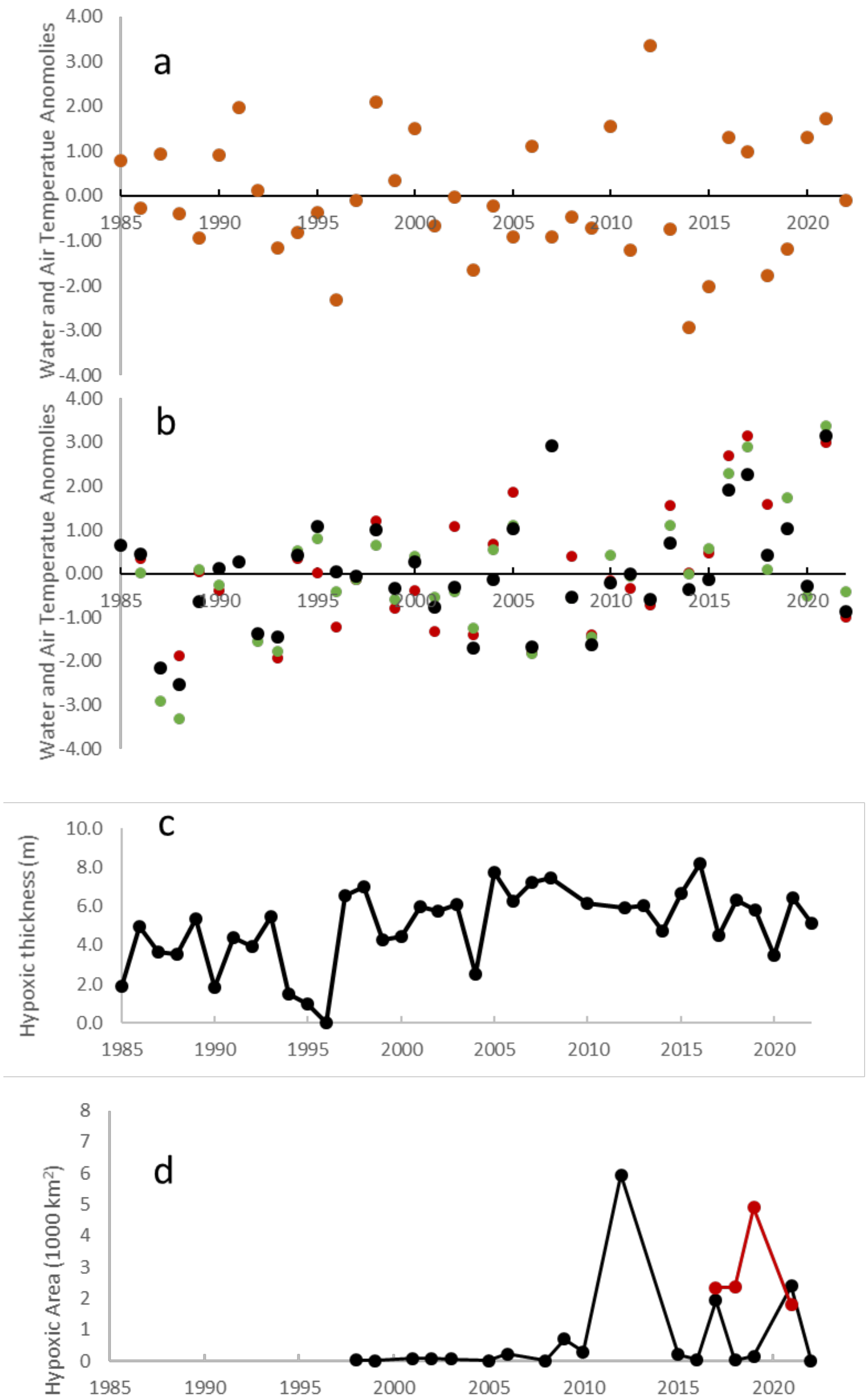

Figure S7. a) March-April air temperature anomalies (°C); b) October water (red) and air (green) temperature anomalies (°C) at NDBC buoy and lake-averaged air temperature anomalies (°C) (black); c) hypoxic layer thickness; and d) hypoxic extent at beginning and ending of hypoxic season. July (black) and October (red).

5. Future air temperature projections from CMIP6

Future air temperature was projected using data from the Coupled Model Intercomparison Project Phase 6 (CMIP6). We employed spatially downscaled air temperatures sourced from the NEX-GDDP-CMIP6 dataset (Thrasher et al., 2022), which utilized the bias correction/spatial disaggregation (BCSD) method to downscale the original global climate model output to a 0.25° resolution on a daily timescale. For the Lake Erie watershed, we specifically selected 15 models from the NEX-GDDP-CMIP6 dataset (table below). This selection process prioritized climate models with an Earth System module when multiple models were available from a modeling center (e.g., GFDL-ESM4 from GFDL).

To account for future socioeconomic pathway uncertainties, we considered three Shared Socioeconomic Pathway (SSP) and emission scenarios: SSP1-2.6 "Sustainability," SSP2-4.5 "Middle-of-the-road," and SSP5-8.5 "Fossil-fueled-development." The air temperature differences among these three scenarios are attributed to differing greenhouse gas emissions levels as per projected climate policies.

We computed the daily average temperature for the entirety of the Lake Erie watershed by averaging the intersecting 0.25° resolution grids (Figure S8). Subsequently, we calculated the average air temperatures for March and April during for the historical period (1950-2014, as defined by CMIP6) and for the future scenarios (2015-2099). To assess long-term impacts of air temperature on hypoxia, we selected 2030-2059 to represent the mid-century and 2070-2099 to represent the late century.

Model name	**Modeling center**	**Nominal resolution**
ACCESS- ESM1-5	Commonwealth Scientific and Industrial Research Organisation, Australia	1.250°x1.875°
BCC-CSM2-MR	Beijing Climate Center, China Meteorological Administration, China	1.125°x1.125°
CanESM5	Canadian Centre for Climate Modelling and Analysis, Canada	2.813°x2.813°
CNRM-ESM2-1	Center National de Recherches Météorologiques–Center Européen de Recherche et de Formation Avancée en Calcul Scientifique, France	1.406°x1.406°
GFDL-ESM4	NOAA/Geophysical Fluid Dynamics Laboratory, USA	1.000°x1.250°
HadGEM3- GC31-LL	Met Office Hadley Center, United Kingdom	1.250°x1.875°
IITM-ESM	Centre for Climate Change Research-Indian Institute of Tropical Meteorology, India	1.915°x1.875°
INM-CM5-0	Institute for Numerical Mathematics, Russia	1.500°x2.000°
IPSL-CM6A-LR	L'Institut Pierre-Simon Laplace, France	1.259°x2.500°
KACE-1-0-G	National Institute of Meteorological Sciences-Korea Meteorological Administration, South Korea	1.250°x1.875°
MIROC-ES2L	Model for Interdisciplinary Research on Climate, Japan	2.813°x2.813°
MPI-ESM1-2- HR	German Climate Computing Centre, Germany	0.938°x0.938°
MRI-ESM2-0	Meteorological Research Institute, Japan	1.125°x1.125°
NESM3	Nanjing University of Information Science and Technology, China	1.875°x1.875°
UKESM1-0-LL	Met Office Hadley Center, United Kingdom	1.250°x1.875°

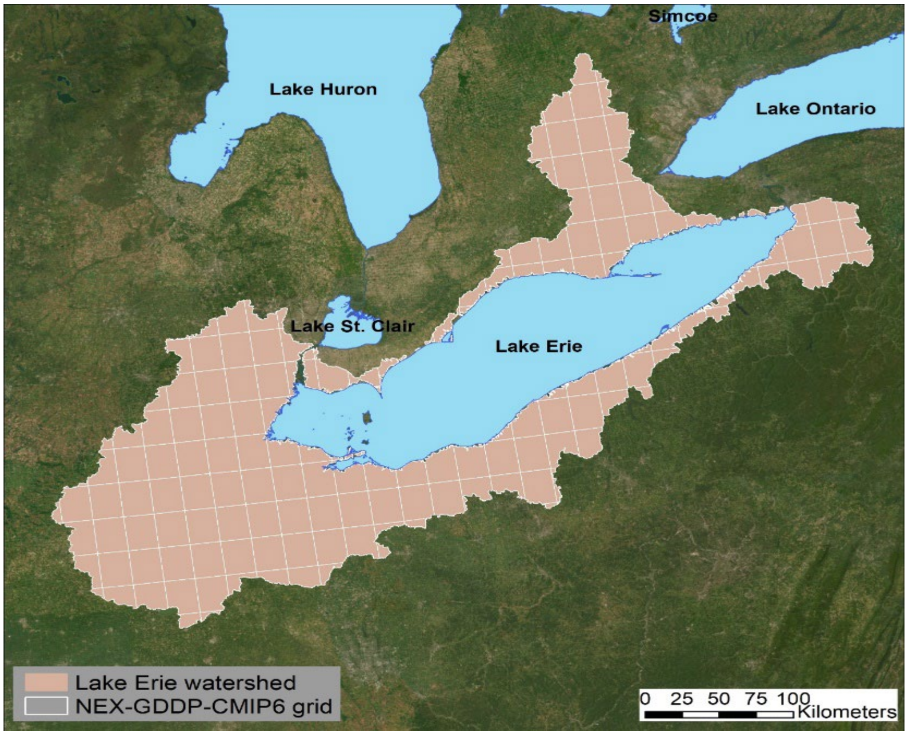

Lake Erie watershed and 0.25° climate model grids from the NEX-GDDP-CMIP6 dataset.

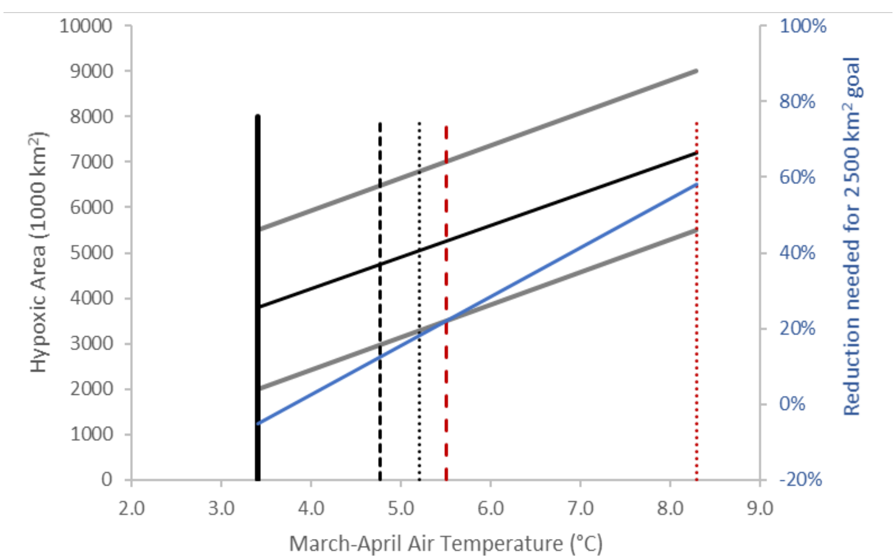

Figure S8. Vertical black lines represent current (solid), mid-century (dashed), and late-century (dotted) conditions for the SSP1-2.6 (black) and SSP5-8.5 (red) scenarios. Mean predicted hypoxic extent (black) and upper and lower 60% confidence intervals (grey) for the 2008 loads. Percent reduction from 2008 required to reach the 4,000 km^2 hypoxia target (blue).

6. Exploration of potential confounding factors of historical variation in fishery harvests

General Overview

The possibility exists that factors besides bottom hypoxia could have driven changes in commercial fishery harvest. The most conspicuous factors include temperature variation (e.g., warming), invasive species (e.g., dreissenid mussels, Rainbow Smelt *Osmerus mordax*, Sea Lamprey *Petromyzon marinus*), and altered regulations on commercial harvest. Below we detail the approach we used to explore the potential for these factors to influence commercial harvest of Lake Whitefish, Walleye, and Yellow Perch. While these additional analyses show that other factors like temperature variation and invasive species appear to have influenced commercial harvest levels, they also support our primary conclusions regarding the impact of hypoxia on commercial harvest. Simply, after accounting for effects of temperature variation and Rainbow Smelt (for all three species), as well as Sea Lamprey (in the case of Lake Whitefish), the hypoxia signal and its associated thresholds remain clear and strong, with hypoxia's importance becoming clearer for Yellow Perch.

Potential Confounding Factors

Lake Erie has been a highly dynamic ecosystem, owing in large part to human-driven environmental change (Hartman, 1972; Fraker et al., 2022; Sinclair et al., 2023). In addition to changes in nutrient availability and associated bottom hypoxia, which is the main focus of this paper, ecosystem change has occurred from the effects of human-driven climate change (e.g., increased warming and springtime precipitation; Farmer et al., 2015; Zhang et al., 2020), the establishment of nuisance invertebrate (e.g., *Dreissena* mussels, predatory zooplankton; Bur et al., 1986; Dermott and Munawar, 1993) and vertebrate (e.g., White Perch *Morone americana*, Sea Lamprey; Lawrie, 1970; Schaeffer and Margraf, 1986) species, and commercial fishery exploitation (Hartman, 1972). Thus, the potential that other factors might be responsible for the observed variation in commercial harvest exists.

Fortunately, a rich literature exists on the impacts of these stressors, which allowed us to determine the timeline of their potential influence on commercial fishery landings. This existing literature helped us eliminate many factors as potential drivers of commercial harvest for all three focal species, reducing the list of potential confounding factors that we needed to explore with quantitative approaches herein. For example, the invasion of invertebrate species, including both dreissenid mussels (zebra mussel *Dreissena polymorpha* and *D. bugensis*; circa 1988) and predatory zooplankton (the spiny water fleas *Bythotrephes longimanus* and *Cercopagis pengoi*; circa 1985 and 2001, respectively), and the establishment of a large population of White Perch (circa 1982-1986), occurred too late in our time-series to have been considered as drivers of the noteworthy reductions in commercial harvest that occurred during the 1950s to 1970s. Thus, we did not explore their impacts any further for any of our focal fishes. Furthermore, while Sea Lamprey are known to prey on Lake Whitefish (Coldwater Task Group, 2024), we also know that Sea Lamprey rarely (if at all) prey on Walleye or Yellow Perch (personal communications and unpublished data from: Andy Cook and Tom MacDougall, Ontario Ministry of Natural Resources and Forestry; Ann Marie Gorman, Travis Hartman, Carey Knight, and Eric Weimer, Ohio Department of Natural Resources; Jason Robinson, New York State Department of Environmental Conservation). Thus, we only explored the impacts of Sea Lamprey on Lake Whitefish commercial fishery landings.

Rainbow Smelt can prey on the larvae of Lake Whitefish (Gorsky and Zydlewski, 2013), may compete with Yellow Perch for prey (Hrabik et al., 1998), and is a known prey item for juvenile and adult Walleye in Lake Erie (Forage Task Group, 2024; Knight and Vondracek, 1993). Thus, fluctuations in Rainbow Smelt abundance could potentially influence commercial harvests and potentially mask the effect of hypoxia, given that previous research has shown Rainbow Smelt to be negatively affected by hypoxia as well (Stone et al., 2020).

Methods

General overview. While most invasive species were eliminated as potential drivers of Lake Whitefish, Walleye, and Yellow Perch commercial landings, owing to their recent establishment in the lake, we still needed to consider:

1) Temperature variation on all three species, given Lake Erie's warming climate and its potential to negatively influence all three species (Collingsworth et al., 2017; Dippold et al., 2020; Farmer et al., 2015),

2) Sea Lamprey on Lake Whitefish.

3) Rainbow Smelt on all three species.

Unfortunately, time-series data for the potentially confounding factors do not exist as far back as our hypoxia and commercial fishing records. To overcome this limitation, we compared the relationships between hypoxia and commercial landings of all three species during the entire time-series (1932-2020, as presented in the main text) with those found during shorter time stanzas (1952-2020 and 1984-2020), accounting for effects of these other potential confounding factors as data permitted. If other factors were more important than hypoxia, or the nature (e.g., shape, threshold values) of the relationship between hypoxia and fisheries harvest varied between time stanzas, our comparative temporal analysis should reveal it (Fraker et al., 2022).

Generalized additive modeling. We quantified the relationship between hypoxia and commercial harvest of all three species using generalized additive models (GAMs; Hastie and Tibshirani, 1987), which allowed us to account for the partial effects of other factors, including temperature variation, Rainbow Smelt, and Sea Lamprey (in the case of Lake Whitefish). While the influence of temperature was included in all analyses, we only could include Rainbow Smet in the two shorter time periods (1952-2020 and 1984-2020; data did not exist before then), with Sea Lamprey only explored in the 1984-2020 models because Sea Lamprey abundance was not indexed until the early 1980s. Prior to this time, however, Lake Erie's Sea Lamprey population was considered small until phosphorus abatement programs implemented during the early 1970s improved water quality during the early 1980s, and in turn Sea Lamprey spawning habitat (Lawrie, 1970; Ludsin et al. 2001; Makarewicz and Betram 1993;). Inherently then, the low abundance of Sea Lamprey prior to the 1980s rules out this species' role in driving declines in commercial harvest observed during the 1950s for Lake Whitefish.

We conducted our GAMs in Statistica (ver. 13.5.0.17, TIBCO Software Inc, Santa Clara, CA) using a Poisson distribution and log-link function, given the skewed nature of our catch data. To minimize overfitting models, we explored the impact of allowing our models to "wiggle" by altering our degrees of freedom (i.e., knots) from 2-4. We found that the models with 2 degrees of freedom captured the nature of the relationships between all variables without sacrificing much in terms of the amount of variation in commercial landings explained.

Predictor datasets. The predictor data for this modeling emanated from multiple sources. Rainbow Smelt data came from the same commercial fishery landings dataset as our focal species (GLFC, 2022). The temperature data were provided by the University of Michigan's GLISA program (https://glisa.umich.edu/), which were modeled back to 1948. Because historical water temperature do not exist lakewide, we used modeled monthly lakewide air temperature data, which other Lake Erie research has shown to sufficiently capture variation in water temperature (Dippold et al. 2020). We conducted preliminary analyses to explore relationships among average monthly temperatures. Finding all seasons to be strongly correlated with the annual mean temperature (S. Ludsin, unpublished data), we used annual mean temperature as a predictor. The Sea Lamprey data came from an assessment of lakewide Sea Lamprey population size (Robinson et al., 2021; Coldwater Task Group, 2024). The first assessments were made in 1980.

The annual commercial harvest of all three species capture a range of ages individuals (Coldwater Task Group, 2024; Walleye Task Group, 2024; Yellow Perch Task Group, 2024). Thus, it is unlikely that any annual habitat feature (predictor in our GAM) would maximally explain commercial landings in that year, and concomitantly, we would expect habitat conditions in the several years prior to be a better predictor of harvest. Thus, we averaged the values of our predictors in our GAMs over a 5-year period, which produced near identical results of similar analyses conducted with averages over short durations (S. Ludsin, unpublished data). A 5-year window also seemed appropriate because age-5 fish are typically a major portion of the commercial harvest for all three species (Coldwater Task Group, 2024; Walleye Task Group, 2024; Yellow Perch Task Group, 2024). Thus, for all predictors, we only included years in which a full 5-years of data could be averaged together.

Results & Discussion

Lake Whitefish. Our GAM supports our primary conclusion that hypoxia has played a key role in driving variation in commercial harvests of Lake Whitefish and Walleye, with a new-found dependence seen for Yellow Perch. For Lake Whitefish analyses across all three time periods (1932-2020, 1952-2020, and 1984-2020), consistent relationships between hypoxia and harvest were found, indicating a negative effect (Table S1; Figure S9-14). Even after accounting for the partial effects of temperature (1932-2020), temperature and rainbow smelt (1952-2020), and temperature, Rainbow Smelt, and Sea Lamprey (1984-2020), hypoxia explained a significant amount of the variation in commercial harvest levels for Lake Whitefish. The relationship between hypoxia and Lake Whitefish harvest was nonlinear, with harvest rates generally declining when hypoxia levels exceeded ~5,000 km^2. Thus, while increased temperatures and reduced populations of Rainbow Smelt and Sea Lamprey all appear to positively influence Lake

Whitefish commercial landings, significant effects of hypoxia were observed. Lake Whitefish harvest peaked at intermediate levels of nutrient-driven hypoxia that align with the threshold values presented in our primary analyses (see Figure 4 in the main text).

Walleye. The GAMs for Walleye allowed us to draw a similar conclusion as for Lake Whitefish. After removing the partial effects of temperature and Rainbow Smelt (positive effect), hypoxia was still found to be strongly, significantly related to Walleye commercial fishery landings (Figures S9-S13, S15). The relationship between hypoxia and Walleye harvest, while non-linear, was less hump-shaped (unimodal) than that for Lake Whitefish (Table S1; Figures S9-S15). Regardless of the time period, a negative effect of hypoxia on Walleye harvest was found, with the hypoxia decline in the same range that we observed in our 2dKS modeling (see Figure 4 in the main text). Thus, we feel confident asserting that hypoxia has influenced Walleye harvests.

Yellow Perch. Our 2dKS analysis of the linkage between hypoxia and Yellow Perch showed no apparent negative effect of hypoxia on commercial harvests (Figure 4 in the main text). GAMs indicate a positive relationship, which we attributed to bottom-up effects between nutrient inputs and Yellow Perch production, given that hypoxia and nutrients are highly correlated. Interestingly, however, our GAMs also revealed a non-linear relationship between hypoxia and Yellow Perch commercial harvest, with harvest rates being maximal in the range of approximately 7,000 to 9,000 km^2 and declining modestly thereafter (Figure S9-S13). This higher threshold value of hypoxia relative to Lake Whitefish and Walleye meshes well with our expected understanding of how hypoxia should influence fisheries production in general (Caddy, 1993) and our understanding of species-specific tolerances of hypoxia (Colby et al., 1972; Ludsin et al., 2001; Oglesby, 1977; Sinclair et al., 2023). Importantly, this relationship still existed even after accounting for the apparent negative influence of warming and Rainbow Smelt on Yellow Perch landings (Table S1).

Conclusions. The results of this supplemental modeling supports our conclusion that variation in bottom hypoxia has been the key factor driving variation in commercial harvest of Lake Whitefish, Walleye, and Yellow Perch over the long-term. While our GAMs also showed other stressors to be important drivers of fisheries harvest, including climate variation and invasive Rainbow Smelt for all three species and Sea Lamprey for Lake Whitefish (likely through predatory effects), the hypoxia signal remained clear (or became clearer in the case of Yellow Perch), regardless of the temporal scope of analysis. Furthermore, while temperature and invasive species may explain episodic/short-term historical variability in the fisheries landings, hypoxia uniquely explains the major, long-term patterns illustrated in Figure 3 (main text), significantly shaping fisheries harvests during Lake Erie's first bout of eutrophication during the 1950s-1970s and its more recent one.

Table S1. Summary of generalized additive modeling (GAM) results designed to explore the importance of bottom hypoxia, temperature variation, and invasive rainbow smelt and sea lamprey on commercial harvests of lake whitefish, Walleye, and Yellow Perch in Lake Erie during three time periods with differing data availability (1932-2020, 1952-2020, and 1984-2020). For each of these three time periods, a GAM was built with hypoxia as the sole predictor and then again with hypoxia and other potential drivers of change. Rainbow smelt data were only available for 1952-2020, whereas sea lamprey data were only available from 1984-2020. The shape of the best fit spline curve for each variable in each model is provided (traced from plots shown in Figure GAM S9-S16), as is a general description of that curve's relationship based on the plot and coefficient (negative, positive, or hump-shaped). Standardized beta coefficients or beta weights (Std. Score), which were calculated by dividing each estimated predictor variable coefficient divided by its standard deviation are presented to allow relative influence of each variable in the model to be more easily assessed. Doing so is necessary as the measurement units for predictor variables in any given model differed. Coefficients of determination (R^2) values are provided for all models. Note that all coefficients presented were statistically significant (all $P <$ 0.0001).

		Hypoxia				Temperature				Rainbow Smelt				Sea Lamprey			
Species	**Period**	Spline	Curve	Std. Score	R^2	Shape	Curve	Std. Score	R^2	Shape	Relationship	Std. Score	R^2	Shape	Curve	Std. Score	R^2
	1932-2020		Neg.	-62.7	0.37												
Lake Whitefish			Neg.	-3.4			Pos.	27.5	0.55								
	1952-2020		Neg.	-24.2	0.50												
			Neg.	-4.4			Pos.	28.9			Neg.	-60.2	0.76				
	1984-2020		Hump	0.2	0.517												
			Hump	6.3			Pos.	7.7			Neg.	-9.1			Pos.	-14.8	0.69
Walleye	1932-2020		Neg.	-105.1	0.47												
			Neg.	-93.0			Pos.	88.3	0.69								
	1952-2020		Neg.	-151.5	0.60												
			Neg.	-118.8			Pos.	80.4			Pos.	67.6	0.77				
	1984-2020		Neg.	-6.6	0.02												
			Neg.	-54.0			Pos.	16.5			Pos.	-58.1	0.49				
Yellow Perch	1932-2020		Pos.	219.9	0.45												
			Pos.	73.2			Neg.	-89.6	0.61								
	1952-2020		Pos.	181.5	0.54												
			Pos.	98.0			Neg.	-88.2			Neg.	-109.4	0.73				
	1984-2020		Pos.	69.6	0.33												
			Pos.	61.5			Neg.	-45.1			Neg.	-37.6	0.62				

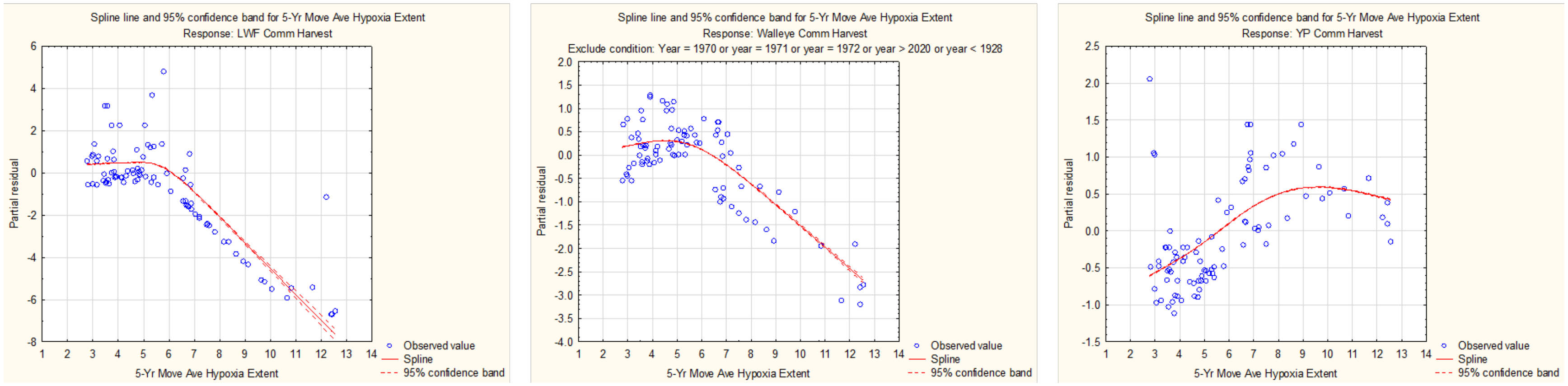

Figure S9. Generalized additive modeling splines with 95% confidence intervals between Lake Whitefish (left), Walleye (middle), and Yellow Perch (right) commercial harvest and the 5-year moving average of modeled annual hypoxia extent, 1932-2020. No other predictors were included in these models. The years 1970-1972 were removed from the analysis of Walleye because commercial fishing did not occur owing to a fishery closure resultant of mercury contamination (GLFC, 2022). See Table S1 for more details about these models.

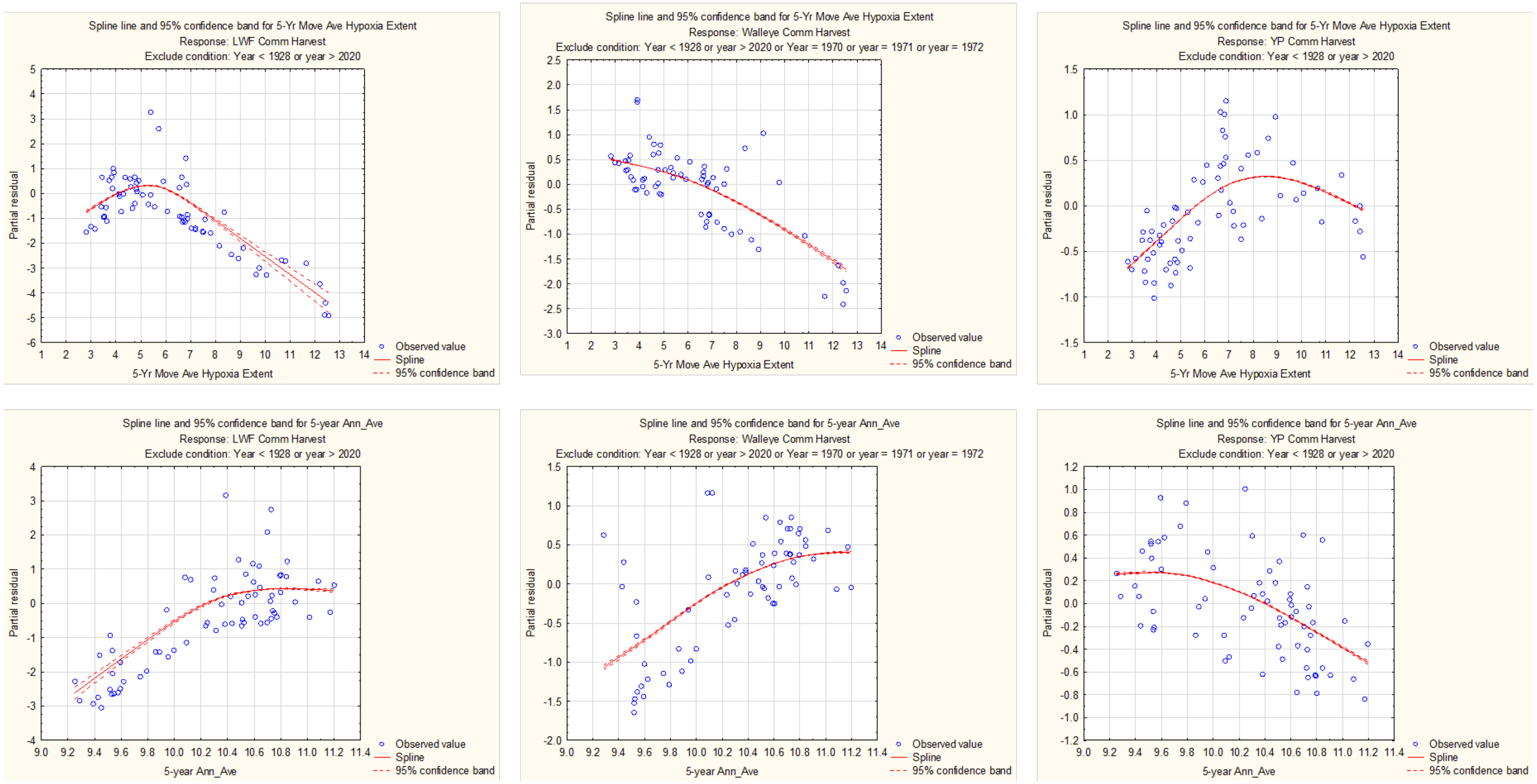

Figure S10. Generalized additive modeling splines with 95% confidence intervals between Lake Whitefish (left), Walleye (middle), and Yellow Perch (right) commercial harvest and the 5-year moving averages of modeled annual hypoxia extent (top panels) and modeled air temperature (bottom panels), 1932-2020. For each spline, variation due to the other predictor variable has been factored out. The years 1970-1972 were removed from the analysis of Walleye because commercial fishing did not occur owing to a fishery closure resultant of mercury contamination (GLFC, 2022). See Table S1 for more details about these models.

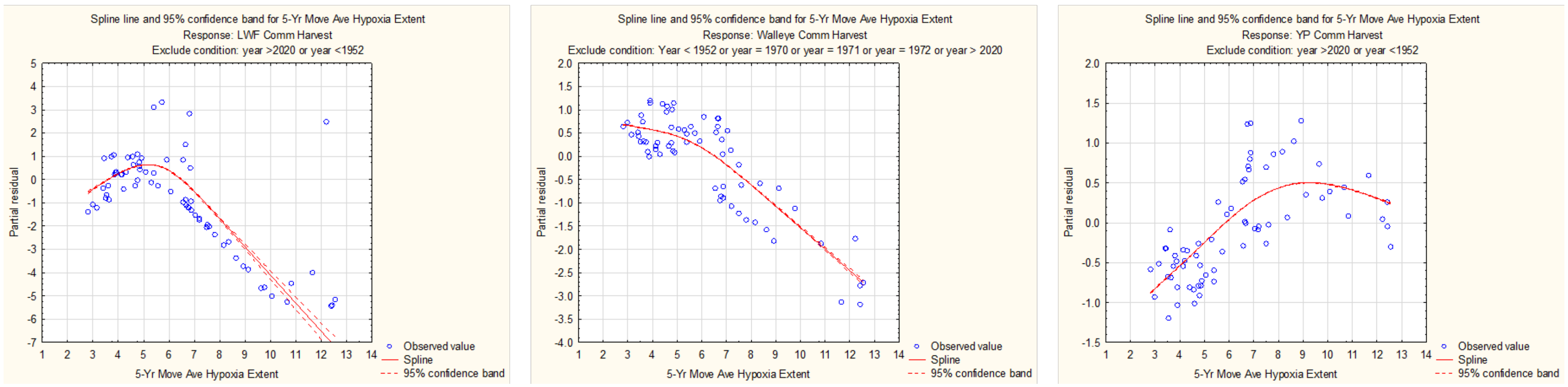

Figure S11. Generalized additive modeling splines with 95% confidence intervals between Lake Whitefish (left), Walleye (middle), and Yellow Perch (right) commercial harvest and the 5-year moving average of modeled annual hypoxia extent, 1952-2020. No other predictors were included in these models. The years 1970-1972 were removed from the analysis of Walleye because commercial fishing did not occur owing to a fishery closure resultant of mercury contamination (GLFC, 2022). See Table S1 for more details about these models.

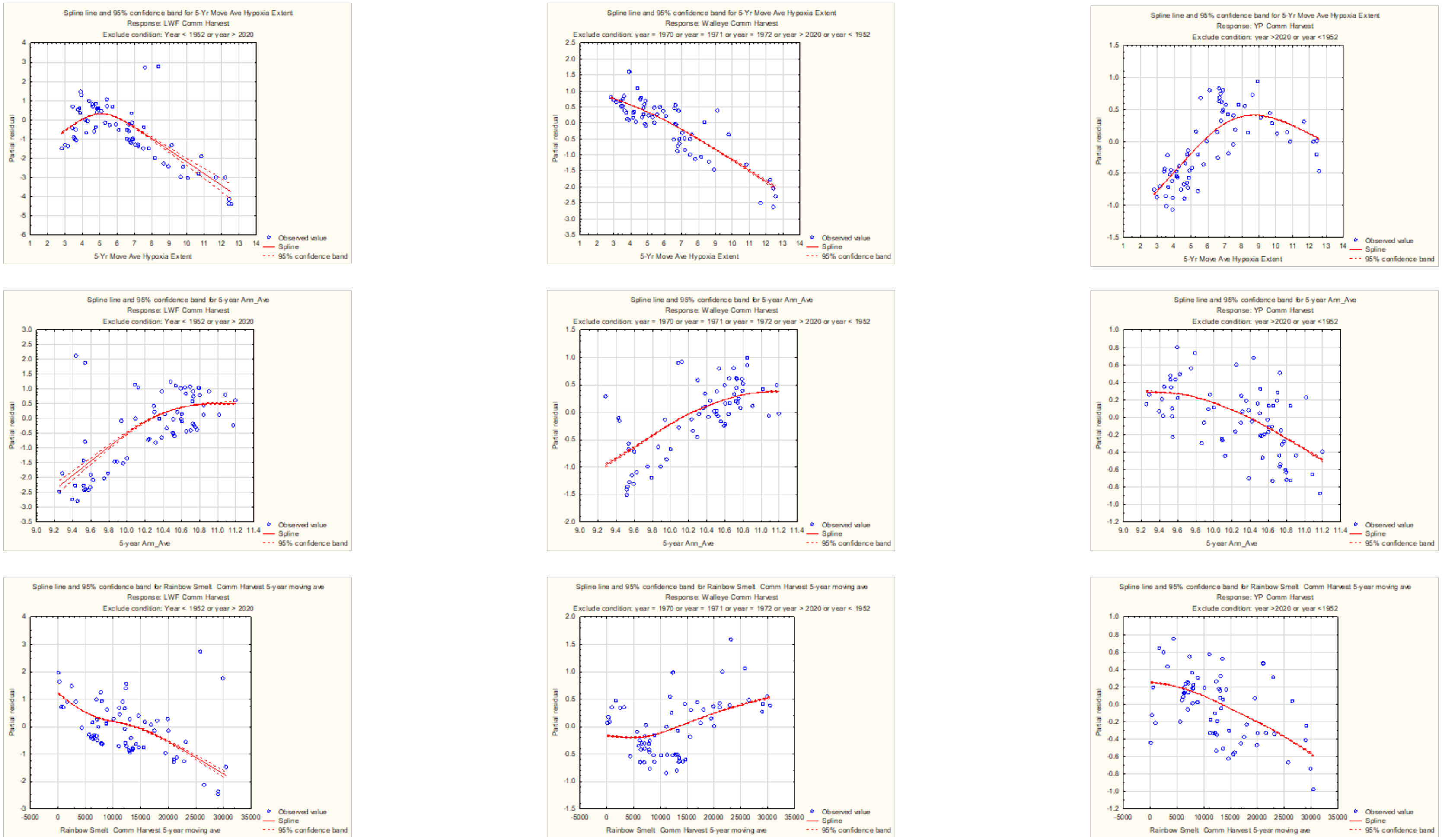

Figure S12. Generalized additive modeling splines with 95% confidence intervals between Lake Whitefish (left), Walleye (middle), and Yellow Perch (right) commercial harvest and the 5-year moving averages of modeled annual hypoxia extent (top panels), modeled air temperature (middle panels), and Rainbow Smelt (bottom panels), 1952-2020. For each spline, variation due to the other predictors variable has been factored out. The years 1970-1972 were removed from the analysis of Walleye because commercial fishing did not occur owing to a fishery closure resultant of mercury contamination (GLFC, 2022). See Table S1 for more details about these models.

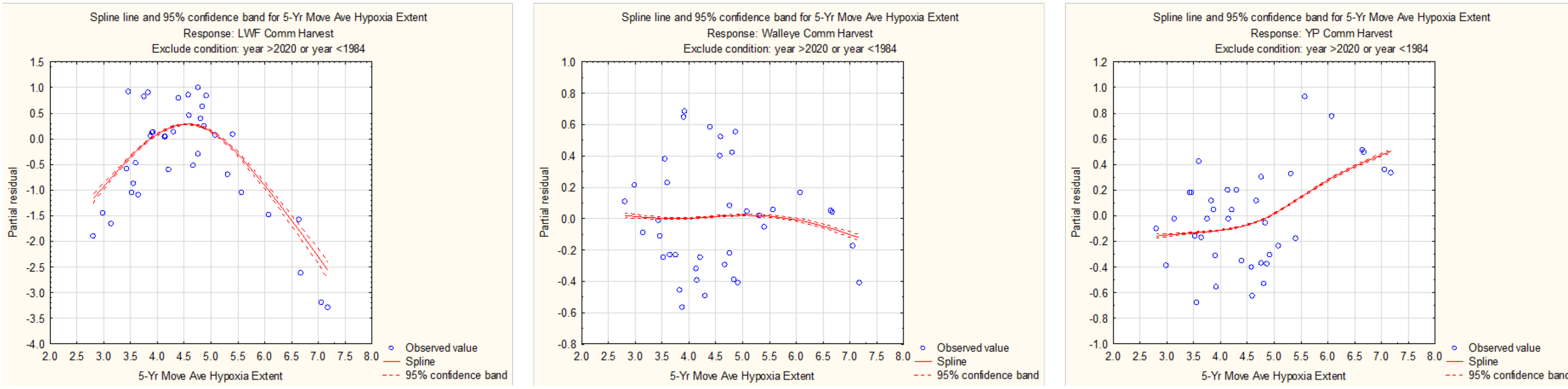

Figure S13. Generalized additive modeling splines with 95% confidence intervals between Lake Whitefish (left), Walleye (middle), and Yellow Perch (right) commercial harvest and the 5-year moving average of modeled annual hypoxia extent, 1984-2020. No other predictors were included in these models. The years 1970-1972 were removed from the analysis of Walleye because commercial fishing did not occur owing to a fishery closure resultant of mercury contamination (GLFC, 2022). See Table S1 for more details about these models.

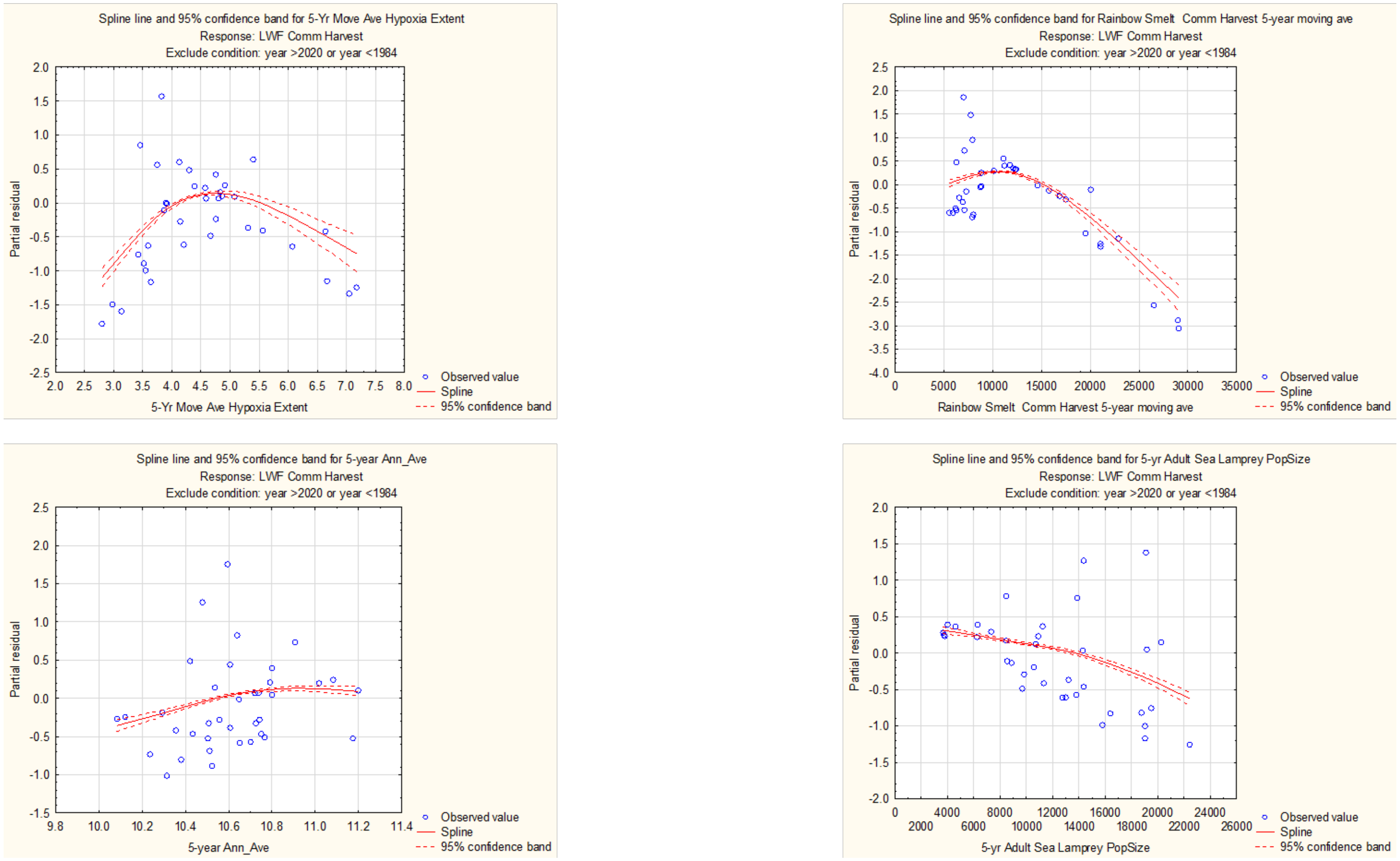

Figure S14. Generalized additive modeling splines with 95% confidence intervals between Lake Whitefish commercial harvest and the 5-year moving averages of modeled annual hypoxia extent (top-left panel), modeled air temperature (bottom-left panel), Rainbow Smelt (top-right panel), and estimated Lake Erie Sea Lamprey population size, 1984-2020. For each spline, variation due to the other predictors variable has been factored out. See Table S1 for more details about these models.

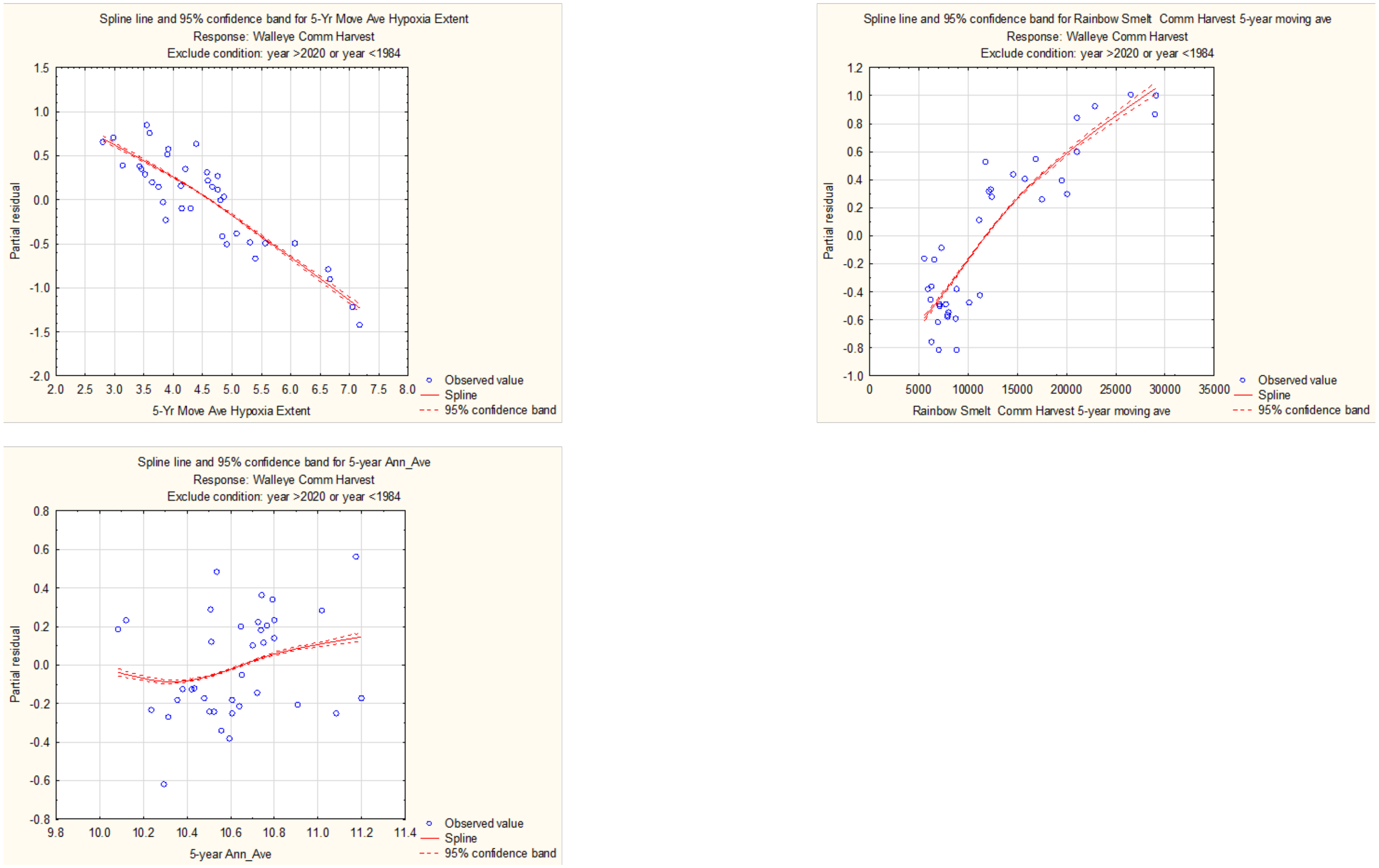

Figure S15. Generalized additive modeling splines with 95% confidence intervals between Walleye commercial harvest and the 5-year moving averages of modeled annual hypoxia extent (top-left panel), modeled air temperature (bottom-left panel), and Rainbow Smelt (top-right panel), 1984-2020. For each spline, variation due to the other predictors variable has been factored out. The years 1970-1972 were removed from the analysis of Walleye because commercial fishing did not occur owing to a fishery closure resultant of mercury contamination (GLFC, 2022). See Table S1 for more details about these models.

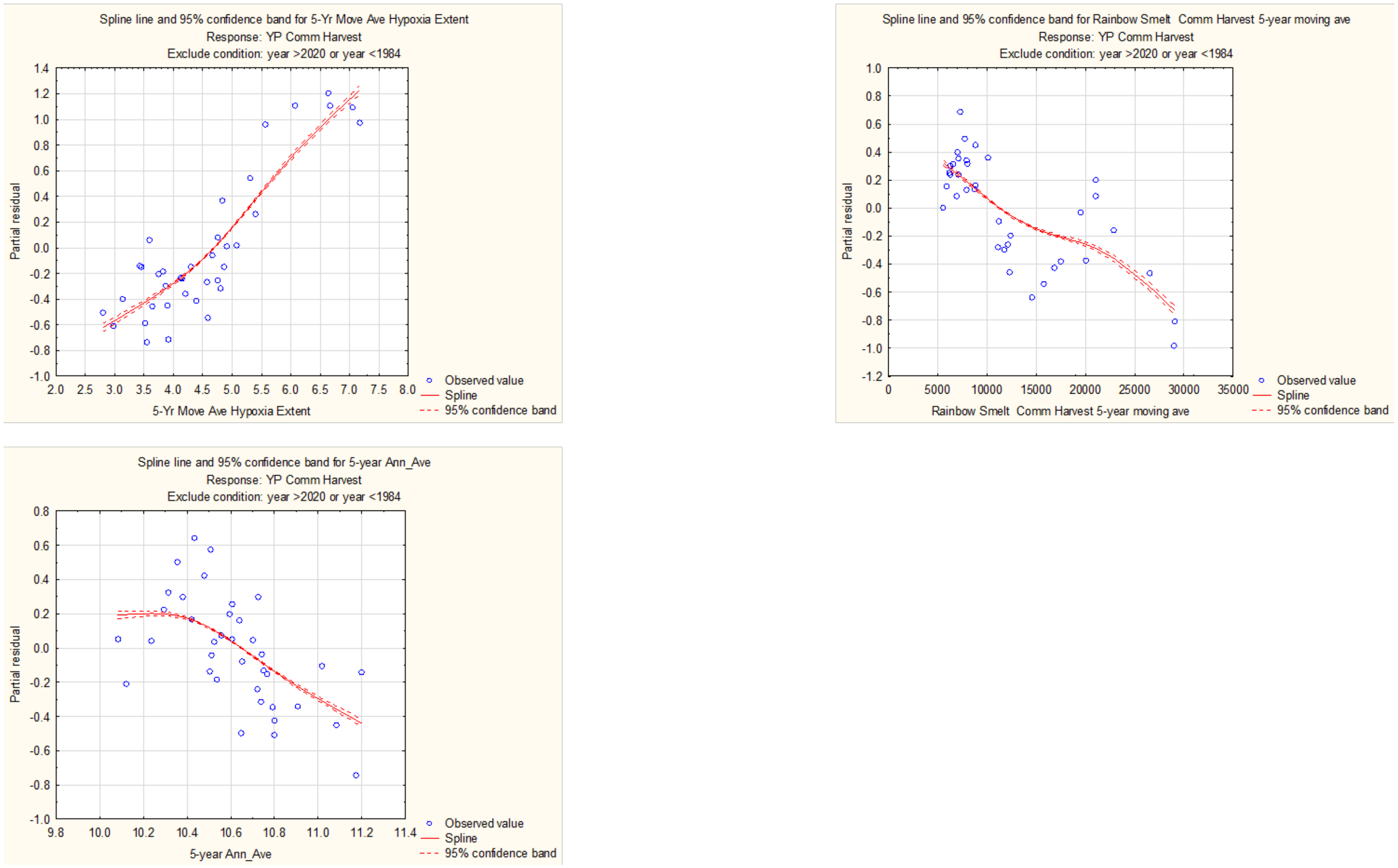

Figure S16. Generalized additive modeling splines with 95% confidence intervals between Yellow Perch commercial harvest and the 5-year moving averages of modeled annual hypoxia extent (top-left panel), modeled air temperature (bottom-left panel), and Rainbow Smelt (top-right panel), 1984-2020. For each spline, variation due to the other predictors variable has been factored out. See Table S1 for more details about these models.

7. Literature Cited

Bur, M.T., Klarer, D.M., Krieger, K.A., 1986. First records of a european cladoceran , *Bythotrephes cederstroemi*, in lakes Erie and Huron, J. Gt. Lakes Res., 12, 144-146.

Caddy, J.F. 1993. Toward a comparative evaluation of human impacts on fishery ecosystems of enclosed and semi-enclosed seas. Rev. Fish. Sci. 1, 57-95.

Colby, P.J., Spangler, G.R., Hurley, D.A., McCombie, A.M., 1972. Effects of eutrophication on salmonid communities in oligotrophic lakes. J. Fish. Res. Board Can. 29, 975-983.

Collingsworth, P.D., Bunnell, D.B., Murray, M.W., Kao, Y.-C., Feiner, Z.S., Claramunt, R.M., Lofgren, B.M., Höök, T.O., Ludsin, S.A., 2017. Climate change as a long-term stressor for the fisheries of the Laurentian Great Lakes of North America. Rev. Fish. Biol. Fish. 27, 363-391.

Coldwater Task Group, 2024. 2023 Report of the Lake Erie Coldwater Task Group, March 2024. Presented to the Standing Technical Committee, Lake Erie Committee of the Great Lakes Fishery Commission, Ann Arbor, MI USA.

Del Giudice, D., Zhou, Y., Sinha, E., Michalak, A.M, 2018. Long-Term Phosphorus Loading and Springtime Temperatures Explain Interannual Variability of Hypoxia in a Large Temperate Lake. Environ, Sci. Technol. 52, 2046-2054.

Dermott, R., Munawar, M., 1993. Invasion of Lake Erie offshore sediments by Dreissena, and its ecological implications. Can. J. Fish Aquat. Sci. 11, 2298-2305.

Di Toro, D.M., Thomas, N.A., Herdendorf, C.E., Winfield, R.P., Connolly, J.P., 1987. A post audit of a Lake Erie eutrophication model. J. Great Lakes Res. 13, 801-825.

Dippold, D.A., Aloysius, N.R., Keitzer, S.C., Yen, H., Arnold, J.G., Daggupati, P., Fraker, M.E., Martin, J.F., Robertson, D.M., Sowa, S.P., 2020. Forecasting the combined effects of anticipated climate change and agricultural conservation practices on fish recruitment dynamics in Lake Erie. Freshw. Biol. 65, 1487-1508.

DiToro, D.M., N.A. Thomas, C.E. Herdendorf, T.P. Winfield, J.P. Connolly. 1987. A post audit of a Lake Erie eutrophication model. J. Great Lakes. Res. 13: 801-825.

Farmer, T.M., Marschall, E.A., Dabrowski, K., Ludsin, S.A., 2015. Short winters threaten temperate fish populations. Nat. Commun. 6.

Forage Task Group, 2024. Report of the Lake Erie Forage Task Group, March 2023. Presented to the Standing Technical Committee, Lake Erie Committee of the Great Lakes Fishery Commission, Ann Arbor, MI USA.

Fraker, M.E., Sinclair, J.S., Frank, K.T., Hood, J.M., Ludsin, S.A., 2022. Temporal scope influences ecosystem driver-response relationships: A case study of Lake Erie with implications for ecosystem-based management. Sci. Tot. Environ. 813, 152473.

GLFC (Great Lakes Fishery Commission). 2022. Commercial fish production in the Great Lakes 1867-2020 [online database]. Great Lakes Fishery Commission, Ann Arbor, MI USA. Available: www.glfc.org/great-lakes-databases.php.

Gorsky, D., Zydlewski, J., 2013. Experimental evaluation of size-dependent predation by adult post-spawned rainbow smelt on larval lake whitefish. N. Am. J. Fish. Manage. 33, 163-169.

Hartman, W.L., 1972. Lake erie: effects of exploitation, environmental changes and new species on the fishery resources. J. Fish. Res. Board Can. 29, 899-912.

Hastie, T., Tibshirani, R., 1987. Generalized additive models: some applications. J. Am. Stat. Assoc. 82, 371-386.

Hrabik, T.R., Magnuson, J.J., McLain, A.S., 1998. Predicting the effects of rainbow smelt on native fishes in small lakes: evidence from long-term research on two lakes. Can. J. Fish. Aquat. Sci 55, 1364-1371.

Lawrie, A., 1970. The sea lamprey in the Great Lakes. Trans. Am. Fish. Soc. 99, 766-775.

Ludsin, S.A., Kershner, M.W., Blocksom, K.A., Knight, R.L., Stein, R.A.,2001. Life after death in Lake Erie: nutrient controls drive fish species richness, rehabilitation. Ecol. Applic. 11, 731-746.

Oglesby, R.T., 1977. Relationships of fish yield to lake phytoplankton standing crop, production, and morphoedaphic factors. J. Fish. Res. Board Can. 34, 2271-2279.

Robinson, K.F., Miehls, S.M., Siefkes, M.J., 2021. Understanding sea lamprey abundances in the Great Lakes prior to broad implementation of sea lamprey control. J. Great Lakes Res., 47, S328-S334.

Rosa, F., N.M. Burns., 1987. Lake Erie central basin oxygen depletion changes from 1929-1980. J. Great Lakes Res. 13: 684-696.

Schaeffer, J.S., Margraf, F.J., 1986. Population characteristics of the invading white perch (*Morone americana*) in western lake erie, J. Great Lakes Res., 12, 127-131.

Sinclair, J.S., Fraker, M.E., Hood, J.M., Reavie, E.D., Ludsin, S.A., 2023. Eutrophication, water quality, and fisheries: a wicked management problem with insights from a century of change in Lake Erie. Ecol. Society 28, 3.

Stone, J.P., Pangle, K.L., Pothoven, S.A., Vanderploeg, H.A., Brandt, S.B., Höök, T.O., Johengen, T.H., Ludsin, S.A., 2020. Hypoxia's impact on pelagic fish populations in Lake Erie: a tale of two planktivores. Can. J. Fish. Aquat. Sci. 77, 1131-1148.

Thrasher, B., Wang, W., Michaelis, A., Melton, F., Lee, T., Nemani, R., 2022. NASA global daily downscaled projections, CMIP6. Sci. Data, 9(1), 262.

Walleye Task Group, 2024. 2023 Report by the Lake Erie Walleye Task Group, March 2024. Presented to the Standing Technical Committee, Lake Erie Committee of the Great Lakes Fishery Commission. Ann Arbor, MI USA.

Yellow Perch Task Group, 2024. Report of the Yellow Perch Task Group, March 2024. Presented to the Standing Technical Committee, Lake Erie Committee of the Great Lakes Fishery Commission. Ann Arbor, MI USA.

Zhang, L., Zhao, Y., Hein-Griggs, D., Janes, T., Tucker, S., Ciborowski, J.J., 2020. Climate change projections of temperature and precipitation for the great lakes basin using the PRECIS regional climate model. J. Great Lakes Res. 46, 255-266.

8. Environmental data used in hypoxia model

Year	Hypoxic Area (1000 km^2)	March-April Air Temperature (°C)	Cumulative TP load (MTA)
1959	7.31	2.48	13204
1960	4.47	1.07	13504
1961	7.36	2.59	13812
1964	9.97	3.26	14776
1970	10.74	1.63	19872
1972	12.11	1.25	21795
1973	15.09	4.91	22713
1974	14.21	3.62	22038
1976	11.45	4.29	18389
1977	6.33	3.59	17107
1978	7.79	1.08	16781
1980	8.22	2.32	14521
1981	8.80	3.27	13810
1982	9.54	2.03	13286
1985	7.37	4.36	11382
1987	7.06	4.51	10525
1988	6.22	3.16	10028
1989	3.12	2.61	9549
1990	5.26	4.48	9565
1991	5.76	5.54	9458
1993	1.93	2.39	9052
1996	0.08	1.24	9145
1997	2.93	3.49	9095
1998	4.60	5.68	9266
1999	3.61	3.93	9195
2000	4.25	5.08	8519
2001	3.88	2.90	8432
2002	2.08	3.54	8544
2003	5.63	1.91	8263
2004	2.37	3.34	7901
2005	3.05	2.65	7836
2006	2.31	4.69	7899
2007	4.04	2.65	8467
2008	5.09	3.07	9107
2010	6.37	5.12	8760
2012	8.52	6.93	8787
2013	5.60	2.82	8628
2014	1.64	0.61	8103
2015	1.82	1.52	7341
2016	2.89	4.88	7280
2017	6.24	4.57	7482
2018	3.28	1.78	7310
2019	3.19	2.36	7635
2020	3.35	4.88	7935
2021	7.92	5.29	7718
2022	5.02	3.45	7845

9. Data used in and fisheries threshold analysis and generalized additive modeling

Year	Lake Whitefish Harvest (1000s of kg)	Walleye Comm Harvest (1000s of kg)	Yellow Perch Comm Harvest (1000s of kg)	5-Yr Moving Ave. of Hypoxia Extent (1000s of km^2)	Rainbow Smelt Harvest (1000s of kg)	5-year Ave. Annual Temperature (°C)	5-yr Adult Sea Lamprey Population Size
1928	1041	596	3903				
1929	1246	423	5322				
1930	1385	857	3520				
1931	1263	1199	6045				
1932	1104	918	6700	2.964			
1933	906	536	2796	3.152			
1934	900	610	9021	2.778			
1935	1160	809	6658	2.993			
1936	1553	1196	1499	3.052			
1937	1087	1388	1561	3.229			
1938	1015	1422	3530	3.565			
1939	2341	2163	1367	3.723			
1940	3066	1755	2278	3.486			
1941	3081	1319	2663	3.568			
1942	2361	1348	1326	4.064			
1943	1290	1462	891	3.789			
1944	970	1587	1615	3.822			
1945	1374	2413	1161	4.725			
1946	1448	2821	2315	5.279			
1947	2388	1775	1836	5.054			
1948	3497	1824	2077	5.330	0		
1949	3767	2410	2240	5.772	0		
1950	1589	2479	2141	5.177	0		
1951	1070	2578	2397	4.982	0		
1952	1476	2335	1789	5.389	375	10.4	
1953	1460	2795	3352	5.735	1030	10.7	
1954	500	2367	5708	5.902	1266	10.6	
1955	410	2628	3248	6.564	2040	10.8	
1956	524	2781	8450	6.644	3694	10.8	
1957	685	2284	9293	6.817	4475	10.7	
1958	297	1796	10193	6.857	4657	10.3	
1959	71	733	13134	6.862	6858	10.2	
1960	20	532	8185	6.546	11496	10.0	
1961	8	365	9516	6.768	12852	10.0	
1962	7	196	12886	6.732	19182	9.8	
1963	10	362	10789	6.885	10830	9.6	
1964	3	256	4477	7.212	13181	9.5	
1965	3	198	9870	7.494	11713	9.5	
1966	5	161	11231	7.795	15923	9.5	
1967	1	232	11545	8.149	12504	9.6	
1968	1	234	12777	8.627	12224	9.7	
1969	1	128	15044	8.927	15078	9.6	

1970	0	11	10444	9.630	9404	9.4	
1971	1	14	7513	10.058	13132	9.4	
1972	1	23	7943	10.656	10521	9.3	
1973	2	29	9034	11.649	17062	9.5	
1974	1	106	6613	12.420	15806	9.6	
1975	1	57	4593	12.407	16934	9.9	
1976	1	115	2962	12.543	17229	9.9	
1977	3	240	5161	12.218	22997	9.9	
1978	2	267	5165	10.826	26630	9.5	
1979	1	542	6893	9.771	23860	9.4	
1980	2	806	7151	9.118	25109	9.3	
1981	11	953	4882	8.343	30326	9.4	
1982	12	917	4424	7.594	43566	9.5	
1983	13	1411	2735	7.511	29494	10.1	
1984	6	1865	4199	7.181	16485	10.5	11283
1985	5	2469	4337	7.046	25478	10.7	12981
1986	9	3054	4991	6.670	17463	10.7	12738
1987	55	3077	5095	6.639	25561	11.0	14276
1988	52	3437	6076	6.073	20404	10.7	14390
1989	61	3120	6355	5.568	16156	10.4	13216
1990	101	3008	4151	5.305	17835	10.6	9835
1991	288	2788	2419	5.401	20221	10.9	8437
1992	292	3086	2318	5.074	12711	10.7	6253
1993	350	4613	1921	4.857	17505	10.7	3652
1994	395	4218	1490	4.809	10593	10.8	3714
1995	421	4504	1265	4.582	12121	10.6	3778
1996	310	4961	1534	3.917	8745	10.1	4597
1997	306	4853	2196	3.899	13062	10.1	4024
1998	537	4687	2061	4.385	14190	10.5	6326
1999	567	4149	1899	4.576	12521	10.8	7293
2000	612	3195	1969	4.757	7162	10.8	11232
2001	542	1720	2140	4.903	9345	11.1	10908
2002	479	1782	2896	4.831	7480	11.2	10719
2003	278	1787	2977	4.137	7395	10.6	8862
2004	285	1279	3161	3.874	12967	10.3	8485
2005	149	2904	3518	3.420	6881	10.4	8537
2006	165	3617	4171	3.594	1847	10.5	10598
2007	420	2623	3515	3.456	9884	10.5	14382
2008	471	2258	2976	3.741	8219	10.6	13863
2009	505	1596	3351	3.820	8068	10.6	19088
2010	310	1485	3601	4.303	3255	10.6	19183
2011	280	2004	3602	4.124	5910	10.4	20229
2012	155	2291	3945	4.757	7452	10.7	19523
2013	72	2065	3393	4.660	6935	10.8	22441
2014	67	2209	3180	4.212	6051	10.5	19054
2015	56	2213	2609	3.509	8333	10.2	18782
2016	25	2271	2579	3.638	10739	10.5	15780
2017	14	2671	2961	3.139	7898	10.3	19060

2018	24	3276	2759	2.802	2558	10.4	16410
2019	52	3579	2008	2.983	1325	10.8	13794
2020	87	4060	1231	3.542	5478	11.2	9667